

A Luminescent Platinum(II) 2,6-Bis(*N*-pyrazolyl)pyridine Complex

Stuart A. Willison, Hershel Jude, Ryan M. Antonelli, Jeffrey M. Rennekamp, Nathan A. Eckert, Jeanette A. Krause Bauer, and William B. Connick*

Department of Chemistry, University of Cincinnati, P.O. Box 210172, Cincinnati, Ohio 45221-0172

Received September 9, 2003

Four platinum(II) cationic complexes were prepared with the *mer*-coordinating tridentate ligands 2,6-bis(*N*-pyrazolyl)pyridine (bpp) and 2,6-bis(3,5-dimethyl-*N*-pyrazolyl)pyridine (bdmpp): [Pt(bpp)Cl]Cl·H₂O; [Pt(bdmpp)Cl]Cl·H₂O; [Pt(bpp)(Ph)](PF₆); [Pt(bdmpp)(Ph)](PF₆). The complexes were characterized by ¹H NMR spectroscopy, elemental analysis, and mass spectrometry, and the structures of the bpp derivatives were determined by X-ray crystallography. [Pt(bpp)Cl]Cl·2H₂O: monoclinic, *P*2₁/*n*, *a* = 11.3218(5) Å, *b* = 6.7716(3) Å, *c* = 20.6501(6) Å, β = 105.883(2)°, *V* = 1522.73(11) Å³, *Z* = 4. The square planar cations stack in a head-to-tail fashion to form a linear chain structure with alternating Pt···Pt distances of 3.39 and 3.41 Å. [Pt(bpp)(Ph)](PF₆)·CH₃CN: triclinic, *P* $\bar{1}$, *a* = 8.3620(3) Å, *b* = 10.7185(4) Å, *c* = 13.4273(5) Å, α = 96.057(1)°, β = 104.175(1)°, γ = 110.046(1)°, *V* = 1072.16(7) Å³, *Z* = 2. Cyclic voltammograms indicate all four complexes undergo irreversible reductions between −1.0 and −1.3 V vs Ag/AgCl (0.1 M TBAPF₆/CH₃CN), attributable to ligand- and/or metal-centered processes. By comparison to related 2,2':6',2''-terpyridine complexes, the electrochemical and UV–visible absorption data are consistent with bpp being both a weaker σ-donor and π-acceptor than terpyridine. Solid samples of [Pt(bpp)(Ph)](PF₆) at 77 K exhibit a remarkably intense, narrow emission centered at 655 nm, whereas the other three complexes exhibit only very weak emission.

Introduction

Since Jameson and Goldsby's report on the regulation of redox potentials of ruthenium(II) complexes with tridentate bis(*N*-pyrazolyl)pyridyl ligands,¹ including bpp and bdmpp, there has been growing interest in using these ligands as easily synthesized substitutes for terpyridyl chelating groups, such as tpy.^{2–5} Whereas luminescent complexes with tpy ligands are well-known,^{6,7} there have been no reports of emissive transition metal complexes with bis(*N*-pyrazolyl)pyridyl ligands. In the case of ruthenium(II) complexes, this result is not surprising since bpp is regarded as both a poorer σ-donor and π-acceptor than tpy.¹ Consequently, complexes such as Ru(bpp)₂²⁺ are expected to have low-lying, triplet ligand field states (³LF) that facilitate rapid nonradiative decay, decreasing the probability of radiative emission. The situation will not necessarily improve for platinum(II) complexes. In fact, low-lying ligand field states have been suggested to account for low quantum yields and short

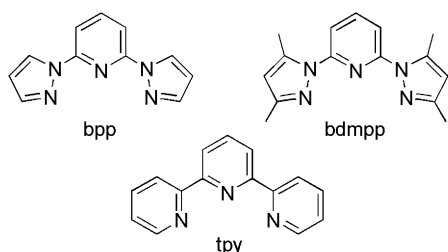
emission lifetimes of some platinum(II) terpyridyl complexes,^{6d,8} though only indirect evidence for these states is presently available. For these reasons, we were surprised to observe intense emission from solid samples of the hexafluoro-

* Author to whom correspondence should be addressed. E-mail: bill.connick@uc.edu.

(1) Jameson, D. J.; Blaho, J. K.; Kruger, K. T.; Goldsby, K. *Inorg. Chem.* **1989**, 28, 4312–4314.

- (2) See for example: (a) Bessel, C. A.; See, R. F.; Jameson, D. L.; Churchill, M. R.; Takeuchi, K. J. *J. Chem. Soc., Dalton Trans.* **1993**, 10, 1563–1576. (b) Fung, W.-H.; Cheng, W.-C.; Yu, W.-Y.; Che, C.-M.; Mak, T. C. W. *Chem. Commun.* **1995**, 2007–2008. (c) Fung, W.-H.; Yu, W.-Y.; Che, C.-M. *J. Org. Chem.* **1998**, 63, 7715–7726. (d) Begley, M. J.; Hubberstey, P.; Stroud, J. J. *J. Chem. Soc., Dalton Trans.* **1996**, 4295–4301. (e) Rülke, R. E.; Kaasjager, V. E.; Kliphuis, D.; Elsevier, C. J.; van Leeuwen, P. W. N. M.; Vrieze, K.; Goubitz, K. *Organometallics* **1996**, 15, 668–677. (f) Holland, J. M.; Kilner, C. A.; Thornton-Pett, M.; Halcrow, M. A. *Polyhedron* **2001**, 20, 2829–2840. (g) Chrysosou, K.; Stergiopoulos, T.; Falaras, P. *Polyhedron* **2002**, 21, 2773–2781. (h) Chrysosou, K.; Catalano, V. J.; Kurtaran, R.; Falaras, P. *Inorg. Chim. Acta* **2002**, 328, 204–209. (i) Calderazzo, F.; Englert, U.; Hu, C.; Marchetti, F.; Pampaloni, G.; Passarelli, V.; Romano, A.; Santi, R. *Inorg. Chim. Acta* **2003**, 344, 197–206. (j) Beach, N. J.; Spivak, G. J. *Inorg. Chim. Acta* **2003**, 343, 244–252. (k) Ayers, T.; Turk, R.; Lane, C.; Goins, J.; Jameson, D.; Slattery, S. J. *Inorg. Chim. Acta* **2004**, 357, 202–206. (3) Bessel, C. A.; See, R. F.; Jameson, D. L.; Churchill, M. R.; Takeuchi, K. J. *J. Chem. Soc., Dalton Trans.* **1991**, 2801–2805. (4) Catalano, V. J.; Kurtaran, R.; Heck, R. A.; Ohman, A.; Hill, M. G. *Inorg. Chim. Acta* **1999**, 286, 181–188. (5) Slattery, S. J.; Bare, W. D.; Jameson, D. L.; Goldsby, K. A. *J. Chem. Soc., Dalton Trans.* **1999**, 1347–1352.

rophosphate salt of Pt(bpp)(Ph)⁺ at 77 K. Here we report the first examples of platinum(II) complexes with bis(*N*-pyrazolyl)pyridyl ligands and their luminescence properties.



Experimental Section

K₂PtCl₄ was purchased from Pressure Chemical, and COD (1,5-cyclooctadiene) was obtained from Aldrich. All other reagents were obtained from Acros. The ligands, 2,6-bis(*N*-pyrazolyl)pyridine (bpp)⁹ and 2,6-bis(3,5-dimethyl-*N*-pyrazolyl)pyridine (bdmpp),⁹ as well as Pt(COD)(Ph)Cl,¹⁰ were prepared according to published procedures. ¹H NMR spectra were recorded at room temperature using a Bruker AC 250 MHz instrument. Deuterated solvents were purchased from Cambridge Isotope Laboratories. Mass spectra were obtained by electrospray ionization using either an Ionspec HiRes ESI-FTICRMS instrument or a Micromass Q-TOF-II instrument. Observed isotope patterns agreed well with predicted patterns on the basis of natural isotopic abundancies. UV–visible absorption spectra were obtained using a HP8453 diode array spectrometer. Elemental analyses were performed by Atlantic Microlab (Norcross, GA). Electrochemical measurements were recorded using a standard three-electrode cell and CV50w potentiostat from Bioanalytical Systems. Scans were recorded in distilled acetonitrile solution containing 0.1 M tetrabutylammonium hexafluorophosphate ((TBA)PF₆), which was recrystallized at least twice from methanol and dried under vacuum prior to use. All scans were recorded using a Pt wire auxiliary electrode, a Ag/AgCl (3.0 M NaCl) reference electrode, and a 0.79 mm² Au working electrode. Reported potentials are referenced vs Ag/AgCl (3.0 M NaCl). Potentials for irreversible reduction couples are reported as the peak potential of the cathodic wave (*E*_{pc}). Reduction of these complexes resulted in a return oxidation wave at positive potentials characteristic of adsorption. Therefore, the working electrode was polished between scans with 0.05 μm alumina, rinsed with distilled water, and dried using a Kimwipe. Steady-state emission data were collected using

a SPEX Fluorolog-3 fluorometer as previously described¹¹ and corrected for instrumental response. Emission samples for lifetime measurements were excited using 4–6 ns pulses from a Continuum Panther optical parametric oscillator (500 nm, <0.3 mJ), pumped with the third harmonic (355 nm) of a Surelite II Nd:YAG laser. Emission transients were detected with a modified PMT connected to a Tektronix TD5580D oscilloscope, and data were modeled by a nonlinear least-squares fitting procedure using in-house software on a Microsoft Excel platform. Time-resolved emission spectra were collected using a similar setup, except the PMT/oscilloscope was replaced with an Andor DH520-25U ICCD (25 mm, 1024 × 256 pixels).

[Pt(bpp)Cl]Cl·H₂O. K₂PtCl₄ (0.50 g, 1.20 mmol) and bpp (0.30 g, 1.42 mmol) were refluxed in water (100 mL) for 4 days. The yellow-tan mixture was filtered, and the filtrate was rotoevaporated to dryness. The yellow solid was washed with ether and hexanes. Yield: 0.484 g (1.01 mmol, 84%). Anal. Calcd for PtC₁₁H₉N₅Cl₂·H₂O: C, 26.68; H, 2.24; N, 14.14. Found: C, 26.57; H, 2.23; N, 14.08. ¹H NMR (CD₃OD, δ): 7.04 (2 H, m), 8.05 (2 H, d, *J* = 3 Hz), 8.13 (2 H, d, *J* = 9 Hz), 8.65 (1 H, t, *J* = 9 Hz), 9.11 (2 H, d, *J* = 4 Hz). MS-ESI (acetonitrile) (*m/z*): 441.014 (Pt(bpp)Cl⁺ calcd 441.019).

[Pt(bdmpp)Cl]Cl·H₂O. This was prepared by the same procedure as for [Pt(bpp)Cl]Cl, substituting the following materials: K₂PtCl₄ (0.250 g, 0.602 mmol); bdmpp (0.193 g, 0.722 mmol); 50 mL of water. Yield: 0.223 g (0.418 mmol, 69%). Anal. Calcd for PtC₁₅H₁₇N₅Cl₂·H₂O: C, 32.68; H, 3.47; N, 12.70. Found: C, 32.43; H, 3.27; N, 12.65. ¹H NMR (CD₃OD, δ): 2.49 (6 H, s), 3.30 (6 H, s), 6.59 (2 H, s), 7.91 (2 H, d, *J* = 9 Hz), 8.51 (1 H, dd, *J* = 9, 9 Hz). MS-ESI (acetonitrile) (*m/z*): 498.077 (Pt(bdmpp)Cl⁺ calcd 498.081).

[Pt(bpp)(Ph)](PF₆). A mixture of 0.246 g (0.592 mmol) of Pt(COD)(Ph)Cl and 0.150 g (0.593 mmol) of AgPF₆ in 10 mL of acetone was stirred at room temperature for 30 min in the dark. The mixture was filtered, and 0.125 g (0.592 mmol) of bpp was added to the filtrate. The pale yellow solution was stirred for 1 day at room temperature and reduced to dryness by rotary evaporation to give a yellow-orange solid. The crude product was recrystallized from acetonitrile and diethyl ether. Yield: 0.247 g (0.393 mmol, 66%). Anal. Calcd for PtC₁₇H₁₄N₅PF₆: C, 32.49; H, 2.25; N, 11.15. Found: C, 32.58; H, 2.25; N, 11.27. ¹H NMR (CD₃CN, δ): 6.89 (2 H, dd, *J* = 3, 3 Hz, with Pt satellites, *J*_{H–Pt} = 16 Hz), 7.18 (3 H, m), 7.49 (2 H, d, *J* = 7 Hz, with Pt satellites, *J*_{H–Pt} = 33 Hz), 7.93 (4 H, m, *J* = 9 Hz), 8.53 (1 H, dd, *J* = 9, 9 Hz), 8.76 (2 H, d, *J* = 3 Hz). MS-ESI (acetonitrile) (*m/z*): 483 (Pt(bpp)(Ph)⁺ calcd 483).

[Pt(bdmpp)(Ph)](PF₆). This was prepared by the same procedure as for [Pt(bpp)(Ph)](PF₆), substituting the following materials: 0.200 g (0.481 mmol) of Pt(COD)(Ph)Cl; 0.122 g (0.483 mmol) of AgPF₆; 10 mL of acetone; 0.129 g (0.483 mmol) of bdmpp. Yield: 0.131 g (0.191 g, 40%). Anal. Calcd for PtC₂₁H₂₂N₅PF₆: C, 36.85; H, 3.24; N, 10.23. Found: C, 36.85; H, 3.11; N, 9.91. ¹H NMR (CD₃CN, δ): 1.71 (6 H, s), 2.78 (6 H, s), 6.31 (2 H, s, with Pt satellites, *J*_{H–Pt} = 19 Hz), 6.96 (1 H, t, *J* = 7 Hz), 7.11 (2 H, dd, *J* = 7, 7 Hz), 7.55 (2 H, d, *J* = 8 Hz, with Pt satellites, *J*_{H–Pt} = 33 Hz), 7.78 (2 H, d, *J* = 8 Hz), 8.35 (1 H, dd, *J* = 9, 9 Hz). MS-ESI (acetonitrile) (*m/z*): 539.155 (Pt(bdmpp)(Ph)⁺ calcd 539.153).

X-ray Crystallography. Crystals of [Pt(bpp)Cl]Cl·2H₂O were grown by slow evaporation of a methanol solution, and intensity data were collected using a Bruker SMART 1K CCD diffractometer.

- (6) See for example: (a) Creutz, C.; Chou, M.; Netzel, T. L.; Okumura, M.; Sutin, N. *J. Am. Chem. Soc.* **1980**, *102*, 1309–1319. (b) Juris, A.; Campagna, S.; Bidd, I.; Lehn, J. M.; Ziessel, R. *Inorg. Chem.* **1988**, *27*, 4007–4011. (c) Ayala, N. P.; Flynn, C. M., Jr.; Sacksteder, L.; Demas, J. N.; DeGraff, B. A. *J. Am. Chem. Soc.* **1990**, *112*, 3837–3844. (d) Aldridge, T. K.; Stacy, E. M.; McMillin, D. R. *Inorg. Chem.* **1994**, *33*, 722–727. (e) Crites Tears, D. K.; McMillin, D. R. *Coord. Chem. Rev.* **2001**, *211*, 195–205.
- (7) Bailey, J. A. H.; Marsh, R. E.; Miskowski, V. M.; Schaefer, W. P.; Gray, H. B. *Inorg. Chem.* **1995**, *34*, 4591–4599.
- (8) (a) Yip, H.-K.; Cheng, L.-K.; Cheung, K. K.; Che, C. M. *J. Chem. Soc., Dalton Trans.* **1993**, 2933–2938. (b) Crites Tears, D. K.; Cunningham, C. T.; McMillin, D. R. *Inorg. Chim. Acta* **1998**, *273*, 346–353. (c) Lai, S.-W.; Chan, M. C. W.; Cheung, K.-K.; Che, C.-M. *Inorg. Chem.* **1999**, *38*, 4262–4267. (d) Michalec, J. F.; Bejune, S. A.; McMillin, D. R. *Inorg. Chem.* **2000**, *39*, 2708–2709. (e) Michalec, J. F.; Bejune, S. A.; Cuttall, D. G.; Summerton, G. C.; Gertenbach, J. A.; Field, J. S.; Haines, R. J.; McMillin, D. R. *Inorg. Chem.* **2001**, *40*, 2193–2200. (f) Yang, Q.-Z.; Wu, L.-Z.; Wu, Z.-X.; Zhang, L.-P.; Tung, C.-H. *Inorg. Chem.* **2002**, *41*, 5653–5655.
- (9) Goldsby, K. A. J.; D. L. *J. Org. Chem.* **1990**, *55*, 4992–4994.
- (10) Eaborn, C. O.; K. J.; Pidcock, A. *J. Chem. Soc., Dalton Trans.* **1978**, 357–368.

- (11) Jude, H.; Krause Bauer, J. A.; Connick, W. B. *Inorg. Chem.* **2002**, *41*, 2275–2281.

Table 1. Crystallographic Data for [Pt(bpp)Cl]Cl·2H₂O and [Pt(bpp)(Ph)](PF₆)·CH₃CN

	[Pt(bpp)Cl]Cl·2H ₂ O	[Pt(bpp)(Ph)](PF ₆)·CH ₃ CN
formula	[C ₁₁ H ₉ N ₅ ClPt]Cl·2H ₂ O	[C ₁₇ H ₁₄ N ₅ Pt]PF ₆ ·CH ₃ CN
fw	513.25	669.45
space group	P2 ₁ /n	P1
a, Å	11.3218(5)	8.3620(3)
b, Å	6.7716(3)	10.7185(4)
c, Å	20.6501(6)	13.4273(5)
α, deg	90	96.057(1)
β, deg	105.883(2)	104.175(1)
γ, deg	90	110.046(1)
V, Å ³	1522.73(11)	1072.16(7)
ρ _{calcd} , g cm ⁻³	2.239	2.074
μ, mm ⁻¹	9.576	6.690
Z	4	2
T, K	150(2)	150(2)
reflens collcd	15 406	14 810
indpnt reflens	3735	5330
R _{int}	0.0591	0.0245
GOF on F ²	1.034	1.040
R1/wR2 [<i>I</i> > 2σ(<i>I</i>)] ^a	0.0310/0.0727	0.0218/0.0498
R1/wR2 (all data) ^a	0.0529/0.0825	0.0277/0.0521

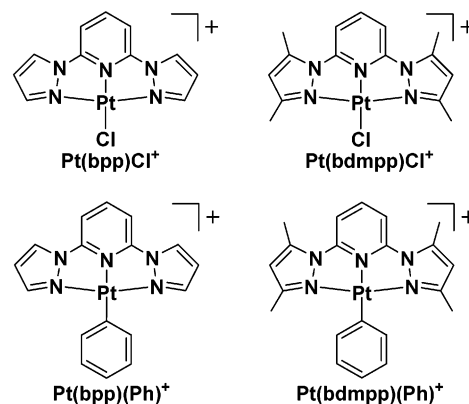
$$^a R1 = \sum |F_o| - |F_c| / \sum |F_o|; wR2 = [\sum w(F_o^2 - F_c^2)^2 / \sum w(F_o^2)^2]^{1/2}.$$

Crystals of [Pt(bpp)(Ph)](PF₆)·CH₃CN were grown by diffusion of ether into an acetonitrile solution, and intensity data were collected using a SMART6000 CCD diffractometer. For both crystals, graphite-monochromated Mo Kα radiation ($\lambda = 0.71073$ Å) was used. Data frames were processed using the SAINT program,¹² and reflection data were corrected for decay, Lorentz, and polarization effects. Absorption and beam corrections were applied on the basis of the multiscan technique using SADABS.¹³ For the chloro complex, the structure was solved by a combination of direct methods using SHELXTL v5.03¹⁴ and the difference Fourier technique. For the phenyl complex, the structure was solved by a combination of the Patterson method using SHELXTL v6.12¹⁴ and the difference Fourier technique. In both cases, the models were refined by full-matrix least squares on *F*². Non-hydrogen atoms were refined with anisotropic parameters. Ligand-based H atoms were located either directly or calculated on the basis of geometric criteria. The isotropic factors for H atoms were defined as 1.2 times *U*_{eq} of the adjacent atom. The water H atoms for [Pt(bpp)Cl]Cl·2H₂O were held fixed where located with minor adjustment to the positions of H30 and H31. The *U*_{iso} was set at 0.05. For [Pt(bpp)(Ph)](PF₆)·CH₃CN, the PF₆[−] counterion shows typical disorder. Crystallographic data are summarized in Table 1.

Results and Discussion

Synthesis and Characterization. The chloride salts of the two chloro complexes, Pt(bpp)Cl⁺ and Pt(bdmpp)Cl⁺, were prepared by refluxing the free bis(*N*-pyrazolyl)pyridine ligands with K₂PtCl₄. The hexafluorophosphate salts of phenyl derivatives, Pt(bpp)(Ph)⁺ and Pt(bdmpp)(Ph)⁺, were

prepared by allowing Pt(COD)(Ph)Cl¹⁰ to react with silver hexafluorophosphate. After removal of silver chloride by filtration, 1 equiv of bpp or bdmp was added to give Pt(bpp)(Ph)⁺ or Pt(bdmpp)(Ph)⁺, respectively. All four compounds gave satisfactory elemental analyses and mass spectra. Both chloro products were found to retain 1 equiv of H₂O with tenacity reminiscent of [Pt(tpy)Cl]Cl·2H₂O.¹⁵ The ¹H NMR spectra exhibit the expected patterns of resonances. For each complex, characteristic doublet and triplet pyridyl proton resonances occur in the ranges of 7.2–8.2 and 8.4–8.7 ppm, respectively. In the case of the bpp complexes, resonances for the β-pyrazolyl protons occur between 6.3 and 7.0 ppm and show only weak splitting. For the phenyl derivatives, resonances for the phenyl protons occur from 6.9 to 7.6 ppm. Distinct Pt satellites are associated with the α-proton resonances (*J*_{Pt–H} = 33 Hz). Surprisingly, Pt satellites also are resolved for the β-pyrazolyl proton resonance in the spectrum of [Pt(bdmpp)(Ph)](PF₆), resulting from four bond coupling (*J*_{Pt–H} = 19 Hz).



Crystal Structures. The molecular structures of the cations Pt(bpp)Cl⁺ and Pt(bpp)(Ph)⁺ were confirmed by X-ray crystallographic studies of crystals of [Pt(bpp)Cl]Cl·2H₂O and [Pt(bpp)(Ph)](PF₆)·CH₃CN at 150 K. ORTEP diagrams are shown in Figures 1 and 2, and data are summarized in Tables 1 and 2.

In both crystals, the bpp ligands adopt a tridentate coordination geometry, bonding to the Pt center through two pyrazolyl N atoms and the pyridine N atom to give a nearly planar Pt(bpp) unit. The fourth coordination site is occupied by the anionic ligand. Bond distances and angles of the cations are normal.¹⁶ The central Pt–N1 distance is shorter than the peripheral Pt–N3 and Pt–N5 distances, as expected for the constrained bite angle of the bpp ligand.⁴ The Pt–N1 distance is shorter for the chloro complex (1.950(4) Å) than for the phenyl derivative (1.999(3) Å), in keeping with the relative trans influence of the anionic ligands. The resulting N3–Pt–N5 angles (chloro, 161.3(2)°; phenyl, 158.7(1)°) lie outside the range observed for Ru(II) complexes with similar ligands (154.9–158.0)°,^{2a–c,3,4} but in the case of the chloro complex, the value is comparable to those observed for Pt(tpy)Cl⁺ salts (CF₃SO₃[−], 161.8(2)°;^{8a} ClO₄[−],

(12) Bruker SMART (v5.051 for [Pt(bppy)Cl]Cl·2H₂O; v5.628 for [Pt(bppy)(Ph)](PF₆)·CH₃CN) and SAINT (v5.A06 for [Pt(bppy)Cl]Cl·2H₂O; v6.28A for [Pt(bppy)(Ph)](PF₆)·CH₃CN) programs were used for data collection and data processing, respectively. Bruker Analytical X-ray Instruments, Inc., Madison, WI.

(13) SADABS was used for the application of semiempirical absorption and beam corrections for the CCD data. G. M. Sheldrick, University of Goettingen, Goettingen, Germany, 1996.

(14) SHELXTL v5.03 ([Pt(bppy)Cl]Cl·2H₂O) and SHELXTL v6.12 ([Pt(bppy)(Ph)](PF₆)·CH₃CN) were used for the structure solutions and generation of figures and tables. G. M. Sheldrick, University of Goettingen, Goettingen, Germany, and Siemens Analytical X-ray Instruments, Inc., Madison, WI.

(15) Howe-Grant, M.; Lippard, S. J. *Inorg. Synth.* **1980**, 20, 101–105.

(16) Bessel, C. A.; See, R. F.; Jameson, D. L.; Churchill, M. R.; Takeuchi, K. J. *J. Chem. Soc., Dalton Trans.* **1992**, 3223–3228.

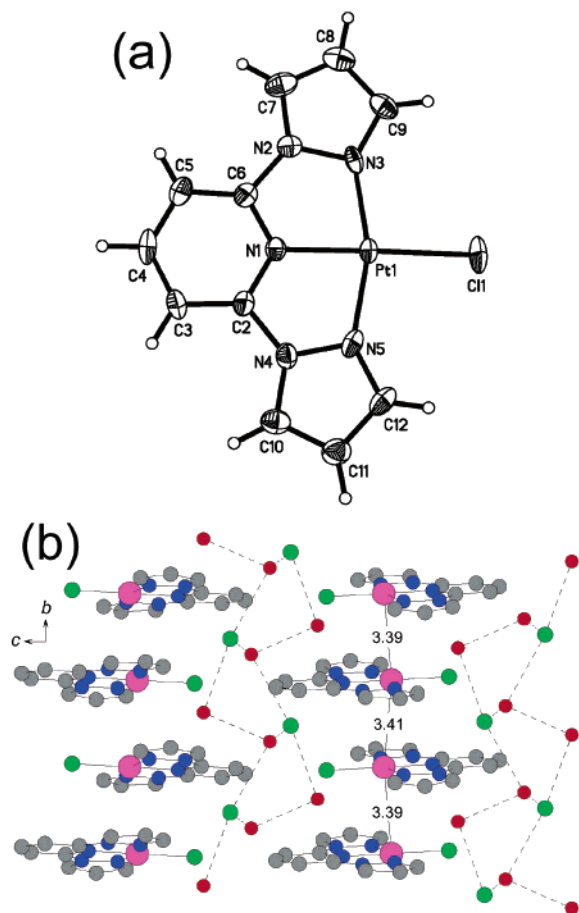


Figure 1. (a) ORTEP diagram of the cation in crystals of $[\text{Pt}(\text{bpp})\text{Cl}]\text{Cl}\cdot 2\text{H}_2\text{O}$ with 50% probability ellipsoids and (b) diagram showing columnar packing parallel to *b* Pt...Pt spacings of 3.39 and 3.41 Å. H-atoms are omitted for clarity.

163.5(7), 161.2(6)°.⁷ Similarly, the N1–Pt–N3 and N1–Pt–N5 angles (79.3–80.7°) for $\text{Pt}(\text{bpp})\text{Cl}^+$ and $\text{Pt}(\text{bpp})(\text{Ph})^+$ are less acute than those generally observed for Ru(II) complexes (77.3–79.6°)^{2a–c,3,4} but smaller than observed for $\text{Pt}(\text{tpy})\text{Cl}^+$ salts (79.8–82.6°),^{7,8a,17} in agreement with the relative ligand bite angles.¹⁶

In crystals of $[\text{Pt}(\text{bpp})\text{Cl}]\text{Cl}\cdot 2\text{H}_2\text{O}$, the approximately square planar $\text{Pt}(\text{bpp})\text{Cl}^+$ cations stack in a head-to-tail fashion to give columns parallel to the *b* axis (Figure 1b). Consecutive complexes along the stack are related by an inversion center, resulting in spacings of approximately 3.33 Å between the coordination planes, defined by the Pt atom and the four coordinating atoms. The stacking arrangement results in a nearly linear chain of Pt atoms (Pt...Pt...Pt, 170.2°) with alternating short Pt...Pt distances (3.39, 3.41 Å) that are characteristic of platinum(II) linear-chain structures with intermolecular metal...metal interactions.¹⁸ The salt crystallizes as a dihydrate, resulting in a hydrogen-bonding network linking the anion and water subunits. The hydrogen-bonding scheme was inferred from short intermolecular contacts between the chloride anion (Cl2) and

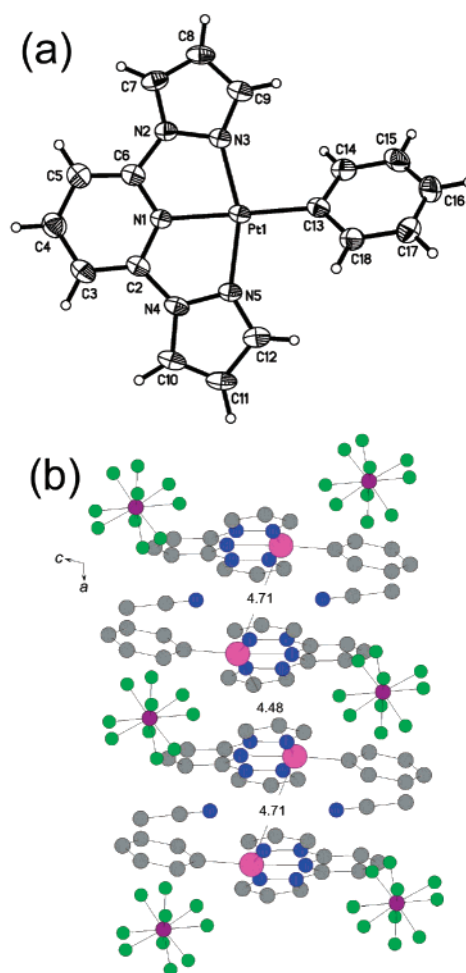


Figure 2. (a) ORTEP diagram of the cation in crystals of $[\text{Pt}(\text{bpp})(\text{Ph})](\text{PF}_6)\cdot \text{CH}_3\text{CN}$ with 50% probability ellipsoids and (b) diagram showing columnar packing parallel to *a* axis with Pt...Pt spacings of 4.48 and 4.71 Å. H-atoms are omitted for clarity.

water O atoms, C12...O1 (3.204(5) Å) and C12...O2 (3.172(5), 3.203(5) Å), as well as between the two water O atoms, O1...O2 (2.982(7) Å). There also are short contacts between the bpp H atoms and the Cl atoms, C4...Cl1 (3.456(6) Å), C5...Cl2 (3.648(6) Å), and C10...Cl1 (3.548(7) Å), as well as between the bpp H atoms and the water groups, C8...O1 (3.423(8) Å), C9...O1 (3.432(8) Å), and C12...O2 (3.483(8) Å).

In crystals of $[\text{Pt}(\text{bpp})(\text{Ph})](\text{PF}_6)\cdot \text{CH}_3\text{CN}$, the $\text{Pt}(\text{bpp})(\text{Ph})^+$ cations also stack in a head-to-tail fashion, forming columns parallel to the *a* axis (Figure 2b). The coordination plane is slightly canted with respect to the *bc* plane, resulting in a 19.3(1)° dihedral angle. Consecutive complexes along the stack are related by an inversion center, resulting in alternating interplanar spacings of ~4.38 and ~4.58 Å. The resulting Pt...Pt separations of 4.48 and 4.71 Å are considerably longer than observed for crystals containing $\text{Pt}(\text{bpp})\text{Cl}^+$. Nevertheless, it is noteworthy that the approximately planar phenyl group forms a 36.9(2)° dihedral angle with the coordination plane. This value lies outside the 55–90° range typically observed for platinum(II) phenyl complexes with bidentate or tridentate ligands.^{19,20} Kaim et. al. have suggested that a dihedral angle of ~60° between the pyridyl and phenyl rings

(17) Wong, Y.-S.; Lippard, S. J. *Chem. Commun.* **1977**, 824–825.
(18) (a) Miller, J. S. *Extended Linear Chain Compounds*; Miller, J. S., Ed.; Plenum Press: New York, 1982; Vols. 1–3. (b) Connick, W. B.; Marsh, R. E.; Schaefer, W. P.; Gray, H. B. *Inorg. Chem.* **1997**, 36, 913–922.

Table 2. Selected Distances (Å) and Angles (deg) for [Pt(bpp)Cl]Cl·2H₂O and [Pt(bpp)(Ph)](PF₆)·CH₃CN

	[Pt(bpp)Cl]Cl·2H ₂ O	[Pt(bpp)(Ph)](PF ₆)·CH ₃ CN
Pt–N1	1.950(4)	1.999(3)
Pt–N3	2.000(5)	2.012(3)
Pt–N5	1.991(5)	2.006(2)
Pt–L ^a	2.298(1)	2.007(3)
N1–C6	1.331(6)	1.334(4)
N1–C2	1.337(7)	1.334(4)
N2–C6	1.421(7)	1.407(4)
N4–C2	1.408(6)	1.402(4)
N2–N3	1.400(6)	1.393(4)
N4–N5	1.391(6)	1.390(4)
N1–Pt–N5	80.6(2)	79.39(10)
N1–Pt–N3	80.7(2)	79.34(10)
N5–Pt–N3	161.3(2)	158.73(11)
N1–Pt–L ^a	178.91(13)	176.38(10)
N5–Pt–L ^a	98.35(14)	101.26(12)
N3–Pt–L ^a	100.34(14)	99.97(11)
C6–N1–Pt	119.3(4)	118.7(2)
C2–N1–Pt	118.7(3)	118.6(2)
N3–N2–C6	118.1(4)	118.7(3)
N5–N4–C2	117.9(4)	119.1(2)
N2–N3–Pt	110.8(3)	111.82(18)
N4–N5–Pt	111.4(3)	111.68(19)

^a L = chlorine (Cl1) for [Pt(bpp)Cl]Cl·2H₂O and carbon (C13) for [Pt(bpp)(Ph)](PF₆)·CH₃CN.

in Pt(diimine)(Ph)₂ complexes provides optimal overlap between the phenyl rings and the π -system of the diimine ligand.²⁰ The angle for Pt(bpp)(Ph)⁺ is remarkably similar to that found for two Pt(Ph)₂ units bridged by 1,2,4,5-tetrakis-(1-N7-azaindolyl)benzene (36.0°), in which intramolecular steric constraints presumably are responsible for the relatively small angle.²¹ Similarly, it is conceivable the relatively acute angle found for Pt(bpp)(Ph)⁺ is a consequence of the compressed columnar packing arrangement of the cations.

Cyclic Voltammetry. To investigate the electronic properties of these complexes, their cyclic voltammograms were recorded in 0.1 M (TBA)PF₆ acetonitrile solution. None of the complexes was oxidized at <1.0 V vs Ag/AgCl. However, all four compounds underwent a chemically irreversible process between –1.0 and –1.3 V (0.25 V/s). Even at 50 V/s, the reductions were completely irreversible. For the chloro complexes, a second irreversible process occurred near –1.45 V. The –1.0 to –1.3 V processes involve reduction of the bis(*N*-pyrazolyl)pyridine ligand and/or reduction of the metal center. Distinguishing between these two possibilities is presently difficult, in part because

the observed processes are irreversible and the E_{pc} values do not necessarily represent thermodynamic potentials. In addition, both the unoccupied ligand π^* and $d_{x^2-y^2}(\text{Pt})$ levels are arguably accessible at these potentials. To illustrate this point, we can obtain crude estimates of the relative orbital energies from accumulated electrochemical data. The cyclic voltammogram of Ru(bpp)₂²⁺ exhibits an irreversible ligand-centered reduction wave at –1.66 V vs SSCE (0.1 M (TBA)PF₆/CH₃CN).¹ Ru(tpy)₂²⁺ is reversibly reduced at more positive potentials (–1.25 V vs SSCE;¹ –1.26 V vs Ag/AgCl (1.0 M KCl), 0.1 M (TBA)PF₆/DMF),²² reflecting the relative energies of the $\pi^*(\text{bpp})$ and $\pi^*(\text{tpy})$ orbitals when bonded to Ru(II).¹ In the case of Pt(tpy)Cl⁺ in DMF, ligand-centered reduction occurs at –0.74 V vs Ag/AgCl (1.0 M KCl).²² Hill and co-workers²² have attributed the 0.52 V anodic shift of the Pt(tpy)Cl⁺ reduction potential with respect to that of Ru(tpy)₂²⁺ to stabilization of the $\pi^*(\text{tpy})$ levels as a result of mixing with the 6p_z(Pt) orbital.²² Similar stabilization of the $\pi^*(\text{bpp})$ level of Pt(bpp)Cl⁺ with respect to Ru(bpp)₂²⁺ would shift the thermodynamic reduction potential of the platinum complex to –1.14 V vs SSCE, in the vicinity of the irreversible reductions observed for this series of platinum(II) bis(*N*-pyrazolyl)pyridyl complexes. On the other hand, Pt(tpy)Cl⁺ undergoes a second chemically reversible reduction in DMF at –1.30 V, generally attributed to addition of an electron to the $d_{x^2-y^2}(\text{Pt})$ orbital.^{22,23} From Hill and co-workers' 0.38 eV estimate for the energy gap between $\pi^*(\text{tpy})$ and $d_{x^2-y^2}(\text{Pt})$ levels²⁴ and assuming similar crystal field strengths, we obtain a crude estimate of –1.12 V vs Ag/AgCl (1.0 M KCl) for the one-electron reduction of the $d_{x^2-y^2}(\text{Pt})$ orbital. The reduction could be expected to occur at even more positive potentials for Pt(bpp)Cl⁺ since bpp is weaker σ -donor than tpy.

Though the observed reductions are irreversible, it is noteworthy that within this series of platinum(II) bis(*N*-pyrazolyl)pyridyl complexes, the peak potentials follow expected trends on the basis of inductive effects, which are expected to shift the energies of the $d_{x^2-y^2}(\text{Pt})$ and $\pi^*(\text{bpp})$ levels in the same direction. Reduction of the bdmpp complexes is slightly less favorable than their bpp counterparts. Similarly, reduction of the phenyl derivatives is ~0.2 V less favorable than the chloro complexes, as expected for the relative donor properties of the ancillary ligands. Overall, the reduction potentials of these complexes are cathodically shifted from those of related Pt(II) terpyridyl complexes,^{8b-d,22,25} including Pt(tpy)(Ph)⁺ (–0.91, –1.42 V vs Ag/AgCl, 1.0 M (TBA)PF₆/CH₃CN),²⁶ in keeping with the

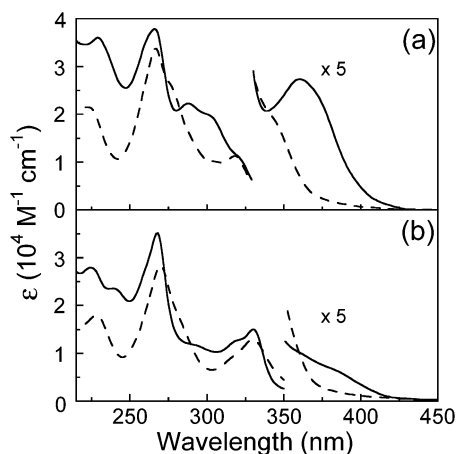
- (19) (a) Bruno, G.; Lanza, S.; Nicolo, F. *Acta Crystallogr.* **1990**, C46, 765–767. (b) Deacon, G. B.; Hilderbrand, E. A.; Tiekink, E. R. T. *Z. Kristallogr.* **1993**, 205, 340–342. (c) Ito, M.; Ebihara, M.; Kawamura, T. *Inorg. Chim. Acta* **1994**, 218, 199–202. (d) Sato, M.; Mogi, E.; Kumakura, S. *Organometallics* **1995**, 14, 3157–3159. (e) Ng, Y.-Y.; Che, C.-M.; Peng, S.-M. *New J. Chem.* **1996**, 20, 781–789. (f) Morton, M. S.; Lachicotte, R. J.; Vivic, D. A.; Jones, W. D. *Organometallics* **1999**, 18, 227–234. (g) Muller, C.; Iverson, C. N.; Lachicotte, R. J.; Jones, W. D. *J. Am. Chem. Soc.* **2001**, 123, 9718–9719. (h) Johansson, M. H.; Malmström, T.; Wendt, O. F. *Inorg. Chim. Acta* **2001**, 316, 149–152. (i) Zucca, A.; Doppiu, A.; Cinellu, M. A.; Stoccoro, S.; Minghetti, G.; Manassero, M. *Organometallics* **2002**, 21, 783–785. (j) Harkins, S. B.; Peters, J. C. *Organometallics* **2002**, 21, 1753–1755. (k) Romeo, R.; Scolaro, L. M.; Plutino, M. R.; Romeo, A.; Nicolo, F.; Del Zotto, A. *Eur. J. Inorg. Chem.* **2002**, 629–638. (20) Klein, A.; McInnes, E. J. L.; Kaim, W. *J. Chem. Soc., Dalton Trans.* **2002**, 2371–2378. (21) Song, D.; Sliwowski, K.; Pang, J.; Wang, S. *Organometallics* **2002**, 21, 4978–4983.

- (22) Hill, M. G.; Bailey, J. A.; Miskowski, V. M.; Gray, H. B. *Inorg. Chem.* **1996**, 35, 4585–4590. (23) Liu, X.; McInnes, E. J. L.; Kilner, C. A.; Thornton-Pett, M.; Halcrow, M. A. *Polyhedron* **2001**, 20, 2889–2900. (24) The $\pi^*(\text{tpy})$ – $d_{x^2-y^2}(\text{Pt})$ energy gap for Pt(tpy)Cl⁺ was estimated in ref 20 from the difference of the first two reduction potentials (0.56 V), crudely corrected for electrostatic effects using the difference between the first two reduction potentials of Ru(bpy)₃²⁺ (0.18 V). (25) (a) Yam, V. W.-W.; Tang, R. P.-L.; Wong, K. M.-C.; Cheung, K.-K. *Organometallics* **2001**, 20, 4476–4482. (b) Jude, H.; Krause Bauer, J. A.; Connick, W. B. *J. Am. Chem. Soc.* **2003**, 125, 3446–3447. (c) Jude, H.; Carroll, G. T.; Connick, W. B. *Chemtracts: Inorg. Chem.* **2003**, 16, 13–22.

Table 3. UV–Visible Absorption^a and Electrochemical Data^b for [Pt(bpp)Cl]Cl, [Pt(bdmpp)Cl]Cl, [Pt(bpp)(Ph)](PF₆), and [Pt(bdmpp)(Ph)](PF₆)

compd	abs λ_{max} , nm (ϵ , cm ⁻¹ M ⁻¹) ^a	E_{pc} , V ^b
bpp	239 (27 700), 245 (34 000), 264 (12 300), 270 sh (11 300), 301 (18 700)	
bdmpp	247 (22 700), 265 sh (11 000), 295 (14 400)	
[Pt(bpp)Cl]Cl	222 (21 500), 267 (33 800), 278 (25 200), 318 (11 300), 340 sh (4100)	-1.07, -1.44
[Pt(bpp)(Ph)](PF ₆)	229 (36 000), 266 (37 800), 288 (22 300), 300 sh (20 000), 320 sh (11 300), 360 (5500)	-1.24
[Pt(bdmpp)Cl]Cl	228 (17 900), 270 (28 400), 316 sh (9100), 330 (12 900)	-1.12, -1.48
[Pt(bdmpp)(Ph)](PF ₆)	224 (27 900), 239 (23 500), 268 (35 100), 295 sh (11 400), 318 sh (12 500), 330 (14 800)	-1.34

^a In methanol solution. ^b Cyclic voltammograms were recorded in 0.1 M (TBA)PF₆/acetonitrile at 0.25 V/s and referenced vs Ag/AgCl (3.0 M NaCl).

**Figure 3.** UV–visible absorption spectra of salts of (a) Pt(bpp)(Cl)⁺ (---) and Pt(bpp)(Ph)⁺ (—) and (b) Pt(bdmpp)(Cl)⁺ (---) and Pt(bdmpp)(Ph)⁺ (—) in methanol solution.

established view that the bpp ligand is a weaker π -acceptor than *tpy*.

Absorption Spectroscopy. The yellow complexes dissolve to give pale yellow methanol solutions, and their UV–visible absorption spectra are reported in Table 3 and Figure 3. The UV region for each complex is dominated by strong absorptions from 230 to 330 nm. The spectra of the free ligands confirm ligand-centered bands occur in this region, though other charge-transfer transitions also may contribute significant intensity. As observed for the four platinum(II) complexes, the spectrum of Ru(bpp)(1,3-dimethyl- β -diketonate)Cl⁺ exhibits an intense absorption near 270 nm ($\sim 27\,000\text{ M}^{-1}\text{ cm}^{-1}$),^{5,27} suggesting this transition is centered on the bis(*N*-pyrazolyl)pyridine ligand.²⁸ For comparison, coordination of 2,2'-bipyridine to an acidic metal center is known to result in intense and structured π - π^* absorption in the vicinity of 290–310 nm that is very different from the spectrum of the free ligand.²⁹ Related transitions in the spectra of all four platinum(II) complexes are expected to be essentially unperturbed by the electronic properties of the monodentate ligand. For the two bdmpp complexes, a band occurs near 330 nm ($12\,000$ – $15\,000\text{ M}^{-1}\text{ cm}^{-1}$) with a shoulder at ~ 317 nm. The relative insensitivity of this band

to the donor properties of the monodentate ligand and to solvent (e.g., Pt(bdmpp)(Ph)⁺: MeOH, 330 nm; CH₂Cl₂, 333 nm) is suggestive of a bdmpp-centered π - π^* transition. The corresponding transition in the bpp complex may occur at shorter wavelengths, possibly associated with the feature near 320 nm, coincident in the spectra of Pt(bpp)Cl⁺ and Pt(bpp)(Ph)⁺.

At longer wavelengths ($\lambda > 330$ nm), the bpp complexes exhibit an additional absorption band, whereas the bdmpp complexes exhibit a tailing absorption profile. For both Pt(bpp)(Ph)⁺ and Pt(bdmpp)(Ph)⁺, the phenyl complexes absorb at longer wavelengths than the chloro adducts. Interpretation is complicated by the prospect that, in addition to bis(*N*-pyrazolyl)pyridine-centered transitions, metal-to-ligand (bis(*N*-pyrazolyl)pyridine) charge transfer (MLCT), chloride or phenyl ligand-to-metal charge-transfer (LMCT), and chloride or phenyl ligand-to-ligand (bis(*N*-pyrazolyl)pyridine) charge transfer (LLCT) transitions can conceivably occur in this region.^{30,31} Additionally, Klein, Zális, van Slageren, Kaim, and co-workers³² have noted that orbital mixing in related platinum(II) complexes can result in excited states with significant admixtures of these states.

The absorption shift to longer wavelengths associated with substitution of the chloro ligand with more electron-releasing phenyl groups is consistent with stabilization of MLCT, LMCT, and LLCT states. In the case of Pt(bpp)(Ph)⁺, a distinct, solvent-sensitive band maximizes at 360 nm (CH₃CN, 359 nm, $7000\text{ M}^{-1}\text{ cm}^{-1}$; CH₂Cl₂, 377 nm, $5800\text{ M}^{-1}\text{ cm}^{-1}$). Though a definitive assignment is not possible, the bandshape is suggestive of vibronic structure, resulting from bis(*N*-pyrazolyl)pyridyl involvement. The bathochromic shift with decreasing solvent polarity and the band intensity resemble the lowest spin-allowed metal-to-ligand(*tpy*) charge-transfer transition of Pt(*tpy*)Cl⁺ (CH₃CN, 377 nm, $2200\text{ M}^{-1}\text{ cm}^{-1}$, 390 sh; CH₂Cl₂, 388 sh, 405 nm).^{8b,d} Thus, in keeping

- (26) Jude, H.; Krause Bauer, J. A.; Connick, W. B. Manuscript in preparation.
- (27) It is assumed the concentration of the solution reported in Figure 3 of ref 5 was 5.5×10^{-5} M.
- (28) A similar band assignment has been made for a Eu(III) and Tb(III) complexes with a related ligand, 2,6-bis(3-carboxy-1-pyrazolyl)pyridine (Remuiñán, M. J.; Román, H.; Alonso, M. T.; Rodríguez-Ubis, J. C. *J. Chem. Soc., Perkins Trans. 2* **1993**, 1099–1102).
- (29) (a) Bray, R. G.; Ferguson, J.; Hawkins, C. *J. Aust. J. Chem.* **1969**, *22*, 2091–2103. (b) Ohno, T.; Kato, S. *Bull. Chem. Soc. Jpn.* **1974**, *47*, 2953–2957.

- (30) The possibility of Pt d \rightarrow p transitions can be excluded on energetic grounds since these transitions in Pt(II) complexes generally occur at wavelengths shorter than 250 nm (Mason, W. R.; Gray, H. B. *J. Am. Chem. Soc.* **1968**, *90*, 5721–5729. Patterson, H. H.; Tewksbury, J. C.; Martin, M.; Krogh-Jespersen, M.-B.; LoMenzo, J. A.; Hooper, H. O.; Viswanath, A. K. *Inorg. Chem.* **1981**, *20*, 2297–2301. Roberts, D. A.; Mason, W. R.; Geoffroy, G. L. *Inorg. Chem.* **1981**, *20*, 789–796. Isci, H.; Mason, W. R. *Inorg. Chem.* **1984**, *23*, 1565–1569. Mason, W. R. *Inorg. Chem.* **1986**, *25*, 2925–2929).
- (31) Triplet components of these charge-transfer transitions and spin-allowed Pt-centered d–d transitions also are candidates but likely to have relatively weak intensities ($<1000\text{ M}^{-1}\text{ cm}^{-1}$).
- (32) (a) Klein, A.; van Slageren, J.; Zális, S. *Eur. J. Inorg. Chem.* **2003**, 1917–1928. (b) Klein, A.; van Slageren, J.; Zális, S. *Inorg. Chem.* **2002**, *41*, 5216–5225. (c) Kaim, W.; Dogan, A.; Wanner, M.; Klein, A.; Tiritiris, I.; Schleid, T.; Stufkens, D. J.; Snoeck, T. L.; McInnes, E. J. L.; Fiedler, J.; Zális, S. *Inorg. Chem.* **2002**, *41*, 4139–4148. (d) van Slageren, J.; Klein, A.; Zális, S. *Coord. Chem. Rev.* **2002**, *230*, 193–211.

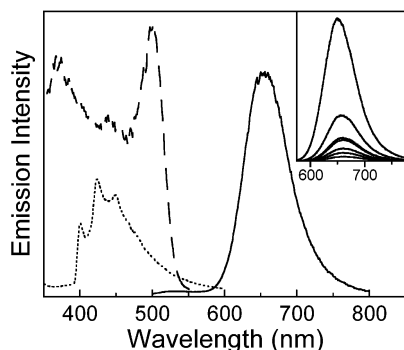


Figure 4. 77 K emission (—, $\lambda_{\text{ex}} = 410$ nm) and excitation (---, $\lambda_{\text{em}} = 640$ nm) spectra of solid $[\text{Pt}(\text{bpp})(\text{Ph})](\text{PF}_6)$ and emission spectrum of a butyronitrile glassy solution (····, $\lambda_{\text{ex}} = 330$ nm). The inset shows time-resolved emission spectra recorded during 90 ns integration windows at 500 ns intervals from 0–4 μs , following a 500 nm excitation pulse.

with the notion of a relatively low-lying unoccupied bpp π^* orbital, this band is tentatively assigned as having significant charge-transfer-to-ligand(bpp) character. The corresponding transition in the spectrum of $\text{Pt}(\text{bpp})\text{Cl}^+$ must occur at wavelengths <345 nm, shifted at least 0.28 eV to the blue of that observed for $\text{Pt}(\text{tpy})\text{Cl}^+$.^{8b,d} For $\text{Pt}(\text{bpp})(\text{Ph})^+$ in alcohol solution, the transition is shifted by ~ 0.5 eV to the blue of that observed for $\text{Pt}(\text{tpy})(\text{Ph})^+$ (4:1 methanol–ethanol, $\lambda_{\text{max}} = 424$ nm, $2000 \text{ M}^{-1} \text{ cm}^{-1}$),³³ in accord with the view that the poorer σ -donor and π -acceptor properties of bpp will tend to destabilize MLCT states. Similar features are less pronounced and apparently weaker in the spectra of $\text{Pt}(\text{bdmpp})(\text{Ph})^+$. However, in CH_2Cl_2 solution, a distinct shoulder is evident near 380 nm ($2000 \text{ M}^{-1} \text{ cm}^{-1}$), suggesting a transition energy similar to that of the bpp complex. Evidently destabilization of the π^* level by the methyl groups of the bdmpp ligand is approximately offset by increased electron donation to the metal center.

Emission Spectroscopy. At room temperature, emissions from samples of each of the four complexes under UV irradiation are exceedingly weak. Even upon cooling to 77 K, salts of $\text{Pt}(\text{bpp})\text{Cl}^+$, $\text{Pt}(\text{bdmpp})(\text{Ph})^+$, and $\text{Pt}(\text{bdmpp})\text{Cl}^+$ only exhibit very weak emissions that could not be reliably recorded. In contrast, the emission from solid $[\text{Pt}(\text{bpp})(\text{Ph})](\text{PF}_6)$ is a remarkably intense pink color at 77 K, and this observation prompted further investigation.

The emission from 77 K solid samples of $[\text{Pt}(\text{bpp})(\text{Ph})](\text{PF}_6)$ is centered at 655 nm (Figure 4). The maximum is independent of excitation wavelength, and the band is nearly symmetrical and relatively narrow as indicated by the full-width at half-maximum (fwhm) of $\sim 1660 \text{ cm}^{-1}$. The excitation spectrum is in *disagreement* with the solution absorption spectrum, showing significant emission intensity for excitation wavelengths as long as 520 nm. Notably, the lowest energy band in the excitation spectrum occurs near 500 nm with an estimated fwhm of $\sim 1200 \text{ cm}^{-1}$. Interestingly, the solid still appeared yellow at 77 K. When the sample was removed from the liquid-nitrogen bath and allowed to warm slightly above 77 K, the emission intensity weakened considerably. Luminescence lifetime measure-

ments show that the 77 K emission signal decay is not single-exponential. The data are adequately described with a biexponential function corresponding to emission lifetimes of approximately 120 and 1550 ns, consistent with a predominantly spin-forbidden process. Despite the complex decay kinetics, time-resolved emission spectra indicate the shape of the emission profile remains essentially constant during the decay, though the maximum undergoes a gradual shift from 650 to 660 nm during the first several hundred nanoseconds (Figure 4). The emission properties of a 10^{-4} M butyronitrile 77 K glassy solution of $\text{Pt}(\text{bpp})(\text{Ph})^+$ are strikingly different. The emission is exceedingly weak but discernibly shifted to much shorter wavelengths ($\lambda_{\text{max}} = 401$, 424, 450 nm; Figure 4) than that of the solid. The apparent vibronic structure with spacings of $\sim 1350 \text{ cm}^{-1}$ is suggestive of emission originating from a lowest ligand-centered $\pi-\pi^*$ state.

The accumulated data are largely consistent with the presence of intermolecular interactions in low-temperature solid samples of $[\text{Pt}(\text{bpp})(\text{Ph})](\text{PF}_6)$ that perturb the emission properties of the complexes. The 77 K emission properties of solid $[\text{Pt}(\text{bpp})(\text{Ph})](\text{PF}_6)$ bear a striking qualitative resemblance to those of dimers^{34,35} and linear chain materials^{8a,36,37} composed of weakly interacting platinum(II) complexes. In these materials, the occupied $5d_{z^2}(\text{Pt})$ orbitals of adjacent complexes interact to form an antibonding ($d\sigma^*$) HOMO, as well as a lower-energy, bonding ($d\sigma$) molecular orbital. Similar interactions between unoccupied $6p_z$ levels of adjacent complexes yields $p\sigma$ and $p\sigma^*$ molecular orbitals, and intense emission from these solids often originates from a lowest $^3(d\sigma^* \rightarrow p\sigma)$ state. In the case of platinum(II) terpyridyl complexes, the LUMO has mostly $\pi^*(\text{tpy})$ character, and the resulting intense emission arises from a lowest $^3(d\sigma^* \rightarrow \pi^*)$ state.³⁶ For both classes of these materials, the ~ 80 K emission profiles tend to be nearly symmetrical with fwhm of $1000\text{--}1600 \text{ cm}^{-1}$.^{8a,34–37} At first glance, either of these excited states seems a tempting candidate for assignment of the emission from $[\text{Pt}(\text{bpp})(\text{Ph})](\text{PF}_6)$.³⁸ The excitation band at 500 nm could be reasonably assigned as the corresponding spin-allowed absorption, which is consistent with typical Stokes shifts and apparent singlet–triplet

(34) Yip, H.-K.; Che, C. M.; Zhou, Z.-Y.; Mak, T. C. W. *J. Chem. Soc., Chem. Commun.* **1992**, 1369–1371.

(35) Bailey, J. A.; Miskowski, V. M.; Gray, H. B. *Inorg. Chem.* **1993**, *32*, 369–370.

(36) (a) Field, J. S.; Haines, R. J.; McMillin, D. R.; Summerton, G. C. *J. Chem. Soc., Dalton Trans.* **2002**, 1369–1376. (b) Field, J. S.; Gertenbach, J.-A.; Haines, R. J.; Ledwaba, L. P.; Mashapa, N. T.; McMillin, D. R.; Munro, O. Q.; Summerton, G. C. *J. Chem. Soc., Dalton Trans.* **2003**, 1176–1180. (c) Büchner, R.; Cunningham, C. T.; Field, J. S.; Haines, R. J.; McMillin, D. R.; Summerton, G. C. *J. Chem. Soc., Dalton Trans.* **1999**, 711–718. (d) Büchner, R.; Field, J. S.; Haines, R. J.; Cunningham, C. T.; McMillin, D. R. *Inorg. Chem.* **1997**, *36*, 3952–3956.

(37) Gliemann, G.; Yersin, H. *Struct. Bonding* **1985**, *62*, 87–153.

(38) The $d\sigma^* \rightarrow \pi^*$ assignment appears more likely since the energies of the emissions from tetracyanoplatinate salts with predominant lowest $d\sigma^* \rightarrow p\sigma$ excited state character only approach that observed here for very short metal···metal spacings $\sim 3.1 \text{ \AA}$.³⁷ The absence of a vibronic component characteristic of ligand excited-state distortion is consistent with the ~ 80 K emission spectra of Pt(II) tpy dimers and linear chain compounds, in which this feature is sometimes, but not always, evident.^{35,36}

(33) Arena, G.; Calogero, G.; Campagna, S.; Scolaro, L. M.; Ricevuto, V.; Romeo, R. *Inorg. Chem.* **1998**, *37*, 2763–2769.

splittings in chain materials.³⁹ However, a troubling inconsistency is the absence of unusually short intermolecular interactions in crystals of [Pt(bpp)(Ph)](PF₆) at 150 K. In fact, the shortest Pt···Pt interactions are considerably longer (4.48, 4.71 Å) than those of crystalline [Pt(bpp)Cl]Cl·2H₂O (3.39, 3.41 Å), which is an exceedingly weak emitter. One possibility is that crystals of [Pt(bpp)(Ph)](PF₆) undergo a phase change below 150 K, resulting in an arrangement of cations having significantly shorter Pt···Pt distances. Indeed, phase changes in linear chain materials are well documented;⁴⁰ however, in the present case there is no corroborating evidence to support this suggestion and further investigation is necessary.

The intense emission from 77 K samples of solid [Pt(bpp)(Ph)](PF₆) contrasts sharply with the relatively broad and weak ³LF emissions observed for many platinum(II) complexes.^{11,41,42} Low-lying LF excited states has been proposed to account for low quantum yields and short emission lifetimes of some platinum(II) terpyridyl complexes,^{6d,8} and a similar explanation for weak emission from several of these platinum(II) bis(*N*-pyrazolyl)pyridyl complexes also may apply. In the case of [Pt(bpp)(Ph)](PF₆), assuming the emission originates from the lowest excited state, we can confidently conclude that the lowest LF states for this complex must be near or at higher energies than the

emission onset ($\leq 16\,900\text{ cm}^{-1}$).⁴³ The relative donor properties of the bpp and tpy ligands suggest that the lowest LF states of platinum(II) terpyridyl complexes are likely to lie at even higher energies than those of related bpp complexes.

Acknowledgment. Diffraction data for [Pt(bpp)Cl]Cl·2H₂O were collected through the Ohio Crystallographic Consortium, funded by the Ohio Board of Regents 1995 Investment Fund (CAP-075) and located at the University of Toledo, Instrumentation Center in A&S, Toledo, OH 43606. We thank the National Science Foundation (Grants CHE-0215950, CHE-0134975) and the University of Cincinnati for support of this research. W.B.C. thanks the Arnold and Mabel Beckman Foundation for a Young Investigator Award. H.J. and W.B.C. are grateful to the University of Cincinnati University Research Council for summer research fellowships. H.J. thanks the University of Cincinnati Department of Chemistry for the Stecker Fellowship, the Link Foundation for an Energy Fellowship, and the University of Cincinnati for a Distinguished Dissertation Fellowship. We thank Drs. M. J. Baldwin, E. Brooks, and K. Jayasimhulu, as well as Mr. Sudhir Shori, for helpful discussions and expert technical assistance.

Supporting Information Available: Tables of crystallographic data, structure refinement details, atomic coordinates, interatomic distances and angles, anisotropic displacement parameters, and calculated hydrogen parameters in CIF format. This material is available free of charge via the Internet at <http://pubs.acs.org>.

IC035066K

(39) Miskowski, V. M.; Houlding, V. H. *Inorg. Chem.* **1991**, *30*, 4446–4452.

(40) Yersin, H.; Gliemann, G.; Råde, H. S. *Chem. Phys. Lett.* **1978**, *54*, 111–116.

(41) Miskowski, V. M.; Houlding, V. H.; Che, C.-M.; Wang, Y. *Inorg. Chem.* **1993**, *32*, 2518–2524.

(42) (a) Yersin, H.; Otto, H.; Zink, J. H.; Gliemann, G. *J. Am. Chem. Soc.* **1980**, *102*, 951–955. (b) Miskowski, V. M.; Houlding, V. H. *Inorg. Chem.* **1989**, *28*, 1529–1533.

(43) The weak emission observed from glassy solutions suggests that the lowest LF states could lie at significantly higher energies ($\geq 25\,000\text{ cm}^{-1}$).